

ESD ACCESSION LIST

XERI Call No. 82807

Copy No. 1 of 2 cys.

Technical Note

1975-19

M. L. Burrows

Performance of the ELF Antenna
Water-Flow Tunnel

27 May 1975

Prepared for the Department of the Navy
under Electronic Systems Division Contract F19628-73-C-0002 by

Lincoln Laboratory

MASSACHUSETTS INSTITUTE OF TECHNOLOGY

LEXINGTON, MASSACHUSETTS



Approved for public release; distribution unlimited.

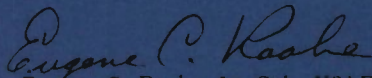
ADA011947

The work reported in this document was performed at Lincoln Laboratory, a center for research operated by Massachusetts Institute of Technology. The work was sponsored by the Department of the Navy under Air Force Contract F19628-73-C-0002.

This report may be reproduced to satisfy needs of U.S. Government agencies.

This technical report has been reviewed and is approved for publication.

FOR THE COMMANDER


Eugene C. Raabe, Lt. Col., USAF

Chief, ESD Lincoln Laboratory Project Office

AD NUMBER

AD-7011947

PAPER COPY

PRICE

\$

DATE

7/8/75

1. REPORT IDENTIFYING INFORMATION

A. ORIGINATING AGENCY

Lincoln Laboratory
Massachusetts Institute of Technology

B. REPORT TITLE AND/OR NUMBER

Technical Note 1975-19

C. MONITOR REPORT NUMBER

ESD-TR-75-172

D. PREPARED UNDER CONTRACT NUMBER(S)

F19628-73-C-0002

2. DISTRIBUTION STATEMENT

"A"

MASSACHUSETTS INSTITUTE OF TECHNOLOGY
LINCOLN LABORATORY

PERFORMANCE OF THE ELF ANTENNA
WATER-FLOW TUNNEL

M. L. BURROWS

Group 61

TECHNICAL NOTE 1975-19

27 MAY 1975

Approved for public release; distribution unlimited.

LEXINGTON

MASSACHUSETTS

ABSTRACT

A water-flow tunnel for testing submarine-towed ELF antennas has been built. A year's operating experience with it shows that it can rapidly provide valuable test data attainable otherwise only slowly on submarines. Its thick aluminum shielding creates, within the tunnel, the electromagnetically quiet undersea environment; the pipe turbulence of the flow excites the antenna cable essentially uniformly along its length, as does the boundary layer turbulence of a cable under tow; and, using a bias winding on the antenna, the axial magnetic bias field can be varied to simulate heading changes.

CONTENTS

Abstract	iii
I. Introduction	1
II. Design Considerations	7
III. Antenna Measurements	15
IV. Measurements of Vibration and Pressure	27
V. Improvements	39
VI. Conclusions	39
Appendix A - Electrical Effect of Tunnel Wall	41
Appendix B - Model Shielding Measurements	44
References	48

Performance of the ELF Antenna Water-Flow Tunnel

I. Introduction

The water-flow tunnel consists of a thick-walled aluminum pipe 110 feet long through which water can be continuously pumped. The antenna cable under test lies under tension in the pipe, and tends to center itself within the pipe when the water is flowing [1]. The tension is required simply to simulate the tension that would exist in the antenna section of a cable under tow. The flow itself keeps the cable roughly centered. The pipe has an internal diameter of 6 inches and an outside diameter of 14 inches. The water flows in a closed loop, the return line being a 10 inch internal diameter thin-walled aluminum pipe.

A sketch and photograph of the tunnel are given in Figs. 1 and 2. The mechanical design has been described in detail by Forman [1].

Since the water-flow tunnel was brought into commission in January 1974, a year's operating experience has been gained with it. Direct measurements of cable vibrations with strain gages have been made, hydrophones at the tunnel wall have been used to measure the pressure fluctuations of the pipe turbulence, the noise voltage generated under various bias conditions by ELF antennas has been investigated and the shielding effectiveness of the tunnel wall has been ascertained. These will be discussed in the following sections.

The water-flow tunnel was built to provide a more accessible and more versatile testing resource than a submarine could provide. At the time the decision was made to go ahead with its procurement, the ELF antenna development program was crippled by a lack of adequate testing. It had been believed

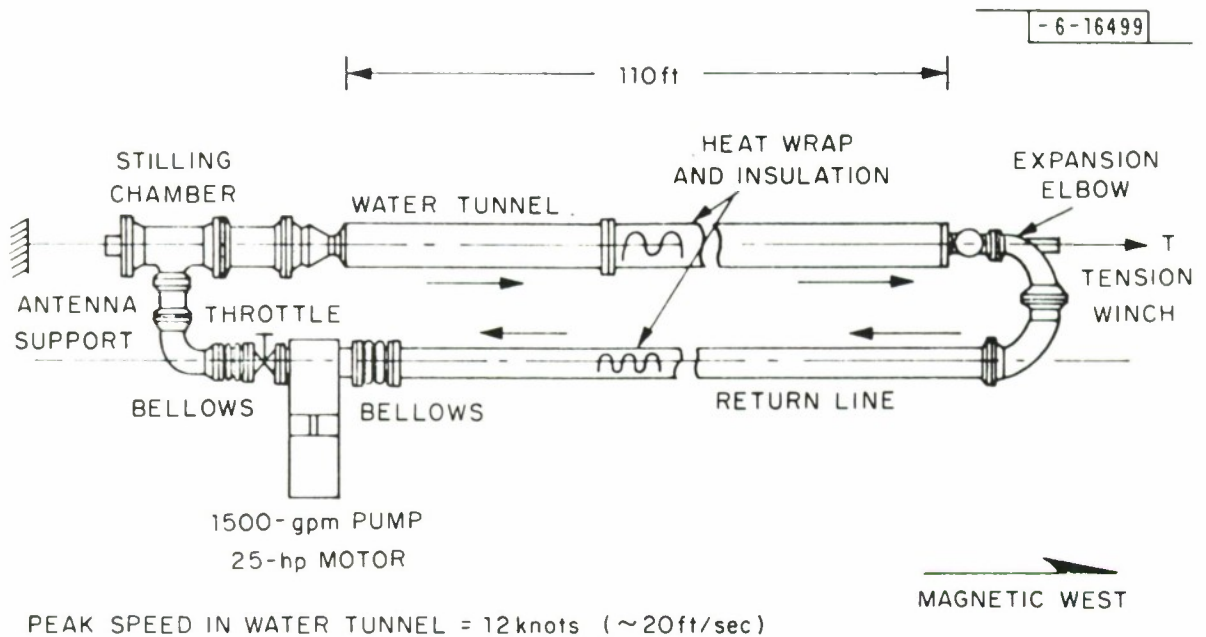


Fig. 1. The ELF antenna water-flow tunnel--a schematic diagram. Access ports [1] are provided at five equally-spaced stations over the length of the 90 ft. test section.

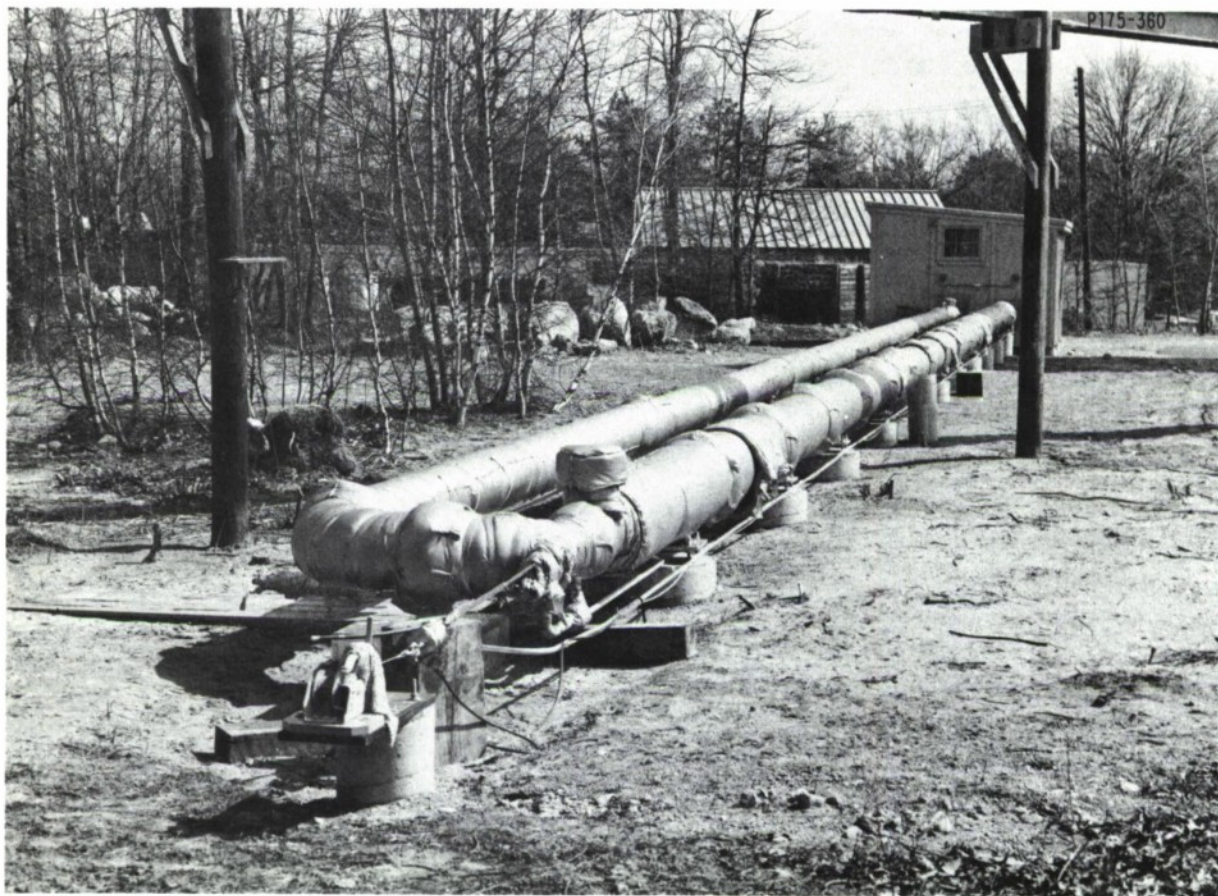


Fig. 2. The ELF antenna water-flow tunnel--a photograph showing the thermally--insulated pipe loop and the pump house. At the near left is the tensioning winch, a load cell and a Kellem's grip on an antenna cable emerging from the tunnel.

that the submarine wake was the main cause of cable vibration, and so it was thought that submarine testing was the only valid way of evaluating the performance of an antenna. Submarines being very difficult to obtain as test vehicles, the development program was in a constant state of delay.

Two advances were responsible for breaking this deadlock. First, measurements with strain gages of the vibration of a submarine-towed antenna cable [2] showed that the excitation is uniform along the length of the cable. And second, a theoretical derivation of the noise voltage spectrum induced in an electrode pair antenna by cable motion excited by the pressure fluctuations in the self-excited turbulent boundary layer of the antenna cable was in close agreement with the directly measured spectrum [3,4]. These two results showed that over the frequency range of interest for ELF communication, the turbulent boundary layer of the cable itself causes the cable vibrations. The role of the submarine is reduced to that of being simply the towing vehicle.

By taking these strain-gage measurements of submarine-towed cable vibration as the basic reference data for cable vibration versus speed, the vibration of any cable of like diameter behind any submarine could now be deduced by simply modifying the original vibration measurements to take account of any differences in cable properties. The formulas connecting surface pressure fluctuations, cable vibration and cable properties have been given in [3].

It is but a small logical extension of this line of reasoning to replace the submarine and the cable's turbulent boundary layer by pumped flow in a pipe or tunnel together with its fully developed pipe turbulence. Once the

cable vibration in the pipe has been measured to be a certain amount more than it would be at the same frequency behind a submarine, then since the relationship between noise and vibration is linear, the antenna noise voltage measured in the pipe will be larger, by the same amount, than it would be behind a submarine. Thus the water-flow tunnel measurement can in principle be used to predict quantitatively the antenna performance behind a submarine.

There remain one or two flies in this ointment. First, there are more than one noise mechanisms, and they arise from different modes of cable vibration [3, 5]. Therefore, if the different modes of cable vibration do not maintain the same relative amplitude levels when the cable is moved from submarine to tunnel, a single scale factor is inadequate to relate the vibration levels. In that case, a separate scale factor must be applied to each vibration mode. It must also be known which noise type is associated with which vibration mode. This in turn requires that there be some theoretical understanding of the noise processes before the tunnel measurements can be meaningful. If the tunnel could be long enough to test a full size antenna, this would be an unfortunate drawback, for the most unambiguous test result is the one requiring the least interpretation. But such a long tunnel is impractical. It would be expensive in shielding material and pump power, and it is unlikely that the cable would keep clear of the tunnel wall unless the tunnel diameter was inordinately large. Thus theoretical interpretation is necessary, in any case, to perform a length scaling from the shorter tunnel-tested antenna to the long version towed behind a submarine. Amplitude scaling then requires no further interpretation and so does not detract further from the tunnel's

utility.

Having the ability to apply the correct scaling presupposes that the amplitude of each significant noise contribution has been evaluated accurately. This is the second fly in the ointment--the problem of discrimination. It is a problem that submarine testing also shares, and for which the problem is in one sense more troublesome. This is because the submarine is less versatile--one cannot, for example, stop the flow and leave everything else unchanged. Even if the captain would agree to stop a submerged submarine, the antenna would neither stay straight nor submerged. The geomagnetic bias condition of the antenna would therefore change also, and in an unpredictable way.

On the other hand, the proportions of the various noise contributions as they occur in a full length submarine towed antenna are realistic. These are the levels that have to be accommodated in the antenna design. But in a short water-flow tunnel, their relative magnitudes might be quite different. In particular, the problem of singling out and measuring a noise contribution which is much smaller in the tunnel, relative to another contribution, than it is in the full length antenna, is correspondingly more difficult. It must be done, however, assuming the noise is a significant contributor to the total noise of the full length antenna, even though it might be an insignificant addition to the total noise of the shorter tunnel-tested antenna. As a subsequent section will show, magnetostrictive noise (also known as stress-induced noise) in the short tunnel-tested antenna tends to obscure the other noise sources, whereas in a long, submarine-tested antenna, motion-induced noise dominates.

The next section will discuss the reasons for choosing the particular length, diameter, water speed and shielding thickness used in building the water tunnel. The sections following that will deal with the results of various measurements made in the tunnel--including those connected with a physical modification made to improve the flow characteristics. A final section discusses future improvements of the tunnel.

II. Design Considerations

Ideally one would like to be able to test full-length antennas in the tunnel. As discussed in the previous section, that is impracticable. So then the question arises of what length is appropriate--which leads to an examination of all the known sources of antenna noise and noting their separate length dependencies.

For a loop antenna with a tapered profile (that is, with sensitivity tapering gradually to zero at each end--see [3]), the power spectral densities of the thermal, magnetostrictive and motion-induced noise voltages are proportional to ℓ , ℓ^2 and ℓ , respectively, provided "profile roughness" is the dominant contributor to motion-induced noise [3]. For motion-induced noise of the "main profile" and "shortness correction" types, the corresponding laws are ℓ^{-1} and ℓ^{-2} , respectively. (To be consistent with the notation used in [3], ℓ stands for the half-length of the antenna.) Thus, even though the "shortness-correction" variety of motion-induced noise might be obscured in a long antenna, its ℓ^{-3} law compared with the "profile-roughness" variety gives it a 30 dB relative enhancement when the antenna length is reduced by a factor of ten. It may well then become highly dominant.

Table I lists the various noise sources and presents numerical estimates of their magnitudes assuming that the frequency is 45 Hz, the tension 150 lb and the cable properties are as given in [3]. The profile roughness noise is estimated on the assumption that for a 1000 ft. long antenna its ENF (Equivalent Noise Field) is only 10 dB greater than the motion-induced ENF of a 1000 ft. electrode-pair antenna, since this seems a reasonable short term goal of the antenna development program. The table includes noise estimates for both a parabolically tapered antenna and a square antenna, both assumed to be of one meter effective (electrical) length. Since the absolute levels of the various noise sources depends on the design of the particular antenna under test, the levels of the four noise sources in a 1000 ft. antenna are denoted symbolically by T, M, S and B.

TABLE I
Numerical Estimates of Antenna Noise Voltage Levels in dBV

Antenna Profile	Antenna Length (ft)	Thermal Noise	Motion-Induced Noise			Magnetostrictive Noise	Barkhausen Noise
			Profile Roughness	Main Profile	Shortness Correction		
Parabolic	1000	T	M	M-21	M-30	S	B
	333	T-5	M-5	M-16	M-20	S+10	B-5
	100	T-10	M-10	M-11	M-10	S+20	B-10
Square	1000	T	M	----	M+21	S+17	B
	333	T-5	M-5	----	M+21	S+17	B-5
	100	T-10	M-10	----	M+21	S+17	B-10

The measurement problem consists of distinguishing between the various noise voltages. For thermal noise, this is straightforward. With no water flow in the tunnel, with the bias field stable and with the core in a demagnetized state, the resulting noise is simply the antenna's thermal noise augmented by the noise figure of the receiver. By sweeping the bias field, still keeping the flow off, Barkhausen noise can be measured. With the flow on and with a large bias field, magnetostrictive noise would be much larger than the thermal or motion-induced noises, and so it can be measured. Finally, with the flow on and the antenna core in a demagnetized state, magnetostrictive noise should be minimized leaving motion-induced noise as the dominant noise. Still, however, there remains the problem of distinguishing between the three forms of motion-induced noise.

Profile roughness noise is the dominant one of these three in a full-length tapered profile antenna. Thus it is the important noise contributor to be measured. Table I shows that it still remains dominant if the antenna length is reduced to 333 ft., but that it merges with the two other motion-induced noises for an antenna of 100 ft. length. However, it is unlikely that the next generation of antennas will have a profile roughness noise only 10 dB greater than the electrode-pair's motion-induced noise. Thus even at 100 ft., profile roughness noise is likely to remain the dominant type of motion-induced noise.

There is no problem of length-enhancement, with respect to profile-roughness noise, of either thermal noise or Barkhausen noise, since all three follow the same length law. Magnetostrictive noise is a completely different

case, however. It is enhanced by 30 dB, compared with profile roughness noise, by shortening the antenna to 100 ft.

The crucial question therefore is whether the theoretical model is accurate enough and whether the experimental demagnetizing procedures are precise enough to reduce the magnetostrictive noise 30 dB more than would be necessary in a 1000 ft. antenna to achieve the same noise discrimination. Experience with short core samples has shown that very deep magnetostrictive nulls are possible. But with short samples, the strain is in-phase along the whole sample length. Even though one part might retain some remanent magnetism in one direction and the other part in the reverse direction, there will exist some bias field at which these cancel perfectly. Then the magnetostrictive noise is strictly zero. A long sample, on the other hand, in which the strain is not in-phase along its whole length, does not possess this property. So an irregular remanence will manifest itself as a magnetostrictive noise floor level that simple bias manipulation will be ineffective in lowering.

Since the cost of a tunnel built to test antennas much in excess of 100 ft. long would have been prohibitive, it was decided that the 100 ft. test antenna length was about the optimum. It was also resolved to take all precautions to facilitate the magnetostrictive minimization. Thus the potential site was surveyed carefully with a magnetometer to make sure no gross magnetic anomaly existed there. The tunnel was laid out perpendicular to the magnetic meridian, and no ferromagnetic material was used in its construction within ten feet of the test section.

If the development program were soon to reduce profile-roughness noise to within 10 dB of the motion-induced noise of the electrode-pair antenna, it could not be measured in the manner suggested above. Table I shows that for a 100 ft. tapered-profile antenna, the profile roughness noise level would then be below the other two motion-induced noise levels. Would this then lead to the tunnel being quickly reduced to obsolescence by advances in antenna design? The square-profile antenna noise estimates given in Table I would appear to allow the answer to this question to be "no". For if the ends of the square profile antenna could be restrained from transverse vibration, the "shortness correction" noise would in principle be zero [3], leaving profile-roughness as the dominant noise source. And the discrimination problem with respect to magnetostrictive noise would be no worse than for a tapered-profile antenna.

Restraining the transverse vibration, an impossibility at sea, is easily effected in the tunnel. Four wires radiating from the cable at each end of the antenna, like spokes from a wheel hub, and attached firmly to the tunnel wall should provide the required degree of restraint while at the same time having negligible effect on the already fully turbulent water flow.

The square-profile antenna has a further attraction as a test sample. Should it prove very difficult to discriminate against magnetostrictive noise in a tapered-profile antenna by simple bias control, the additional method is available of restraining the ends of a square-profile antenna from moving in a longitudinal direction. Since it is the net strain of the whole antenna core that is the effective source, magnetostrictive noise has the same end-

effect quality in a square-profile antenna that motion-induced noise does.

Adopting an antenna length of 100 ft., therefore, enables testing of the present and next generation of antennas to be carried out simply using tapered profiles. It is much less expensive than a full length tunnel would be, and methods exist for extending its utility into the period when profile-roughness noise is much lower than it is today.

There are strong disadvantages in going much below 100 ft. First, the simple scaling laws depend upon $k_t \ell$ and $k_\ell \ell$ being large. (k_t and k_ℓ are the wavenumbers for transverse and longitudinal cable vibration[3]). Also, since profile-roughness noise is measurable only statistically, the antenna sample needs to be long enough to represent a statistically significant sample of the profile of antennas of this design. If some non-uniformity in excitation exists at the inlet end to the tunnel, the tunnel needs to be long enough for the disturbance not to propagate into the antenna region of the cable.

The only advantage in adopting a tunnel length smaller than 100 ft. is the reduced cost of installation. But the 100 ft. length is already reaching the point of diminishing return. The work and cost involved in building a 100 ft. system is not substantially more than that involved in a 50 ft. system, but the utility of the resulting test facility is very much more.

In fact, due to a final trade-off between function and cost, the finished length of the test section is 90 ft. and the shielded section gross length is 110 ft.

The diameter of the water-flow tunnel was determined by the need on the one hand to keep the antenna cable in a region of essentially homogeneous turbulence and to minimize the electrical effect of the massive short circuited

turn that the shielding wall represents. Both of these pointed to a large tunnel diameter. On the other hand, the pumping power required to maintain a certain flow velocity in a pipe is proportional to the pipe-diameter, as is also--approximately--the weight of shielding material required to achieve a given shielding factor. From the results of model experiments on the centering tendency of a cable in coaxial pipe flow [1] and from the results of a theoretical study on the electrical effect of the tunnel walls (see Appendix A), a diameter sized to be hydrodynamically, electrically and economically acceptable was settled upon. It is 6 inches.

Originally it was thought that adequate shielding could be achieved by simply abutting tandem sections of thick walled aluminum pipe. Aluminum was chosen because a given shielding factor could be obtained with aluminum more cheaply than with any other non-ferrous metal. Ferromagnetic materials were not considered for the job, in spite of their better shielding properties, because of the distortion they would induce in the geomagnetic field. The thick walled aluminum tube concept was employed in the final design, but a special overlapped joint was developed to shield against alternating magnetic fields with direction vectors perpendicular to the tunnel axis. Since the antenna is never perfectly straight and coaxial in the tunnel, it can pick up interference due to fields penetrating the shielding in a transverse direction. But the antenna's angular departure from a parallel axis position is never likely to exceed, say 5 or 6°, which means that the shielding of a transverse magnetic field should be within 20 dB of the shielding of a longitudinal magnetic field. Model measurements show that the overlapped joint

design used meets the requirements.

The minimum shielding required for longitudinal fields was determined by the need for the tunnel to simulate the electromagnetic quiet of the ocean at operational antenna depths at frequencies down to 30 Hz. At 400 ft. antenna depth, the depth attenuation at 30 Hz is about 23 dB. However, since the antenna noise level must be some 20 dB below atmospheric noise level at this depth (to facilitate the non-linear noise processing used in proposed ELF receivers, such as the project Sanguine receiver), and since man-made interference may be greater than atmospheric noise, it was judged that a 50 dB shielding factor at 30 Hz would be appropriate.

The four-inch-thick walls of the tunnel achieve this. The measured shielding factor at 60 Hz is 76 dB for longitudinal magnetic fields, which implies a 30 Hz shielding factor of some 53 dB, since theory and the model experiments show shielding factor, in dB, to be proportional to the square root of frequency. Appendix B summarizes the results of the model experiments, including the measurements of shielding against transverse magnetic fields.

The water speed in the tunnel was chosen as a compromise between a large speed which would excite the antenna cable vigorously, thereby generating vibration noises standing well above thermal noise or interference, and a small speed which would require less pumping power. (Pumping power is proportional to speed cubed.) It was, in the end, the power available from a particular electrical supply that determined the final speed of around 10 to 12 knots.

Since the cable excitation in the tunnel arises from the pipe turbulence, it is likely to produce a larger cable vibration at a given speed than the excitation at sea, which arises from the cable's own turbulent boundary layer. Thus there seems no benefit to be derived from driving the water at a speed equal to any particular submarine speed.

III. Antenna Measurements

The water-flow tunnel has two more or less distinct functions within its overall purpose of aiding in the development of a submarine-towed ELF loop antenna. These are, first, being a research facility for exploring the physics of antenna noise generation and second, as a testing instrument for evaluating the various noise levels of a particular candidate antenna design.

In its noise physics role, the water-flow tunnel has allowed, for the first time, direct observation of the four separate noises under towing conditions. These noises are thermal, Barkhausen, motion-induced and magnetostrictive. Figure 3 shows, with the pump off, the thermal noise of the antenna/receiver combination with the antenna core in the demagnetized state and also the Barkhausen noise bursts generated when the antenna core is subjected to a cyclically swept bias field as it would when the towing submarine turns. Figure 4 shows, with the pump on, the motion-induced noise of the antenna as it vibrates in the geomagnetic field with its core demagnetized, and, when the core bias is cyclically swept, it shows Barkhausen noise bursts rising above a magnetostrictive noise background. (In view of the reduced receiver gain in Fig. 4(b), this background is much higher than the motion-induced noise of Fig. 4(a), or the thermal noise of Fig. 3(a) or the thermal

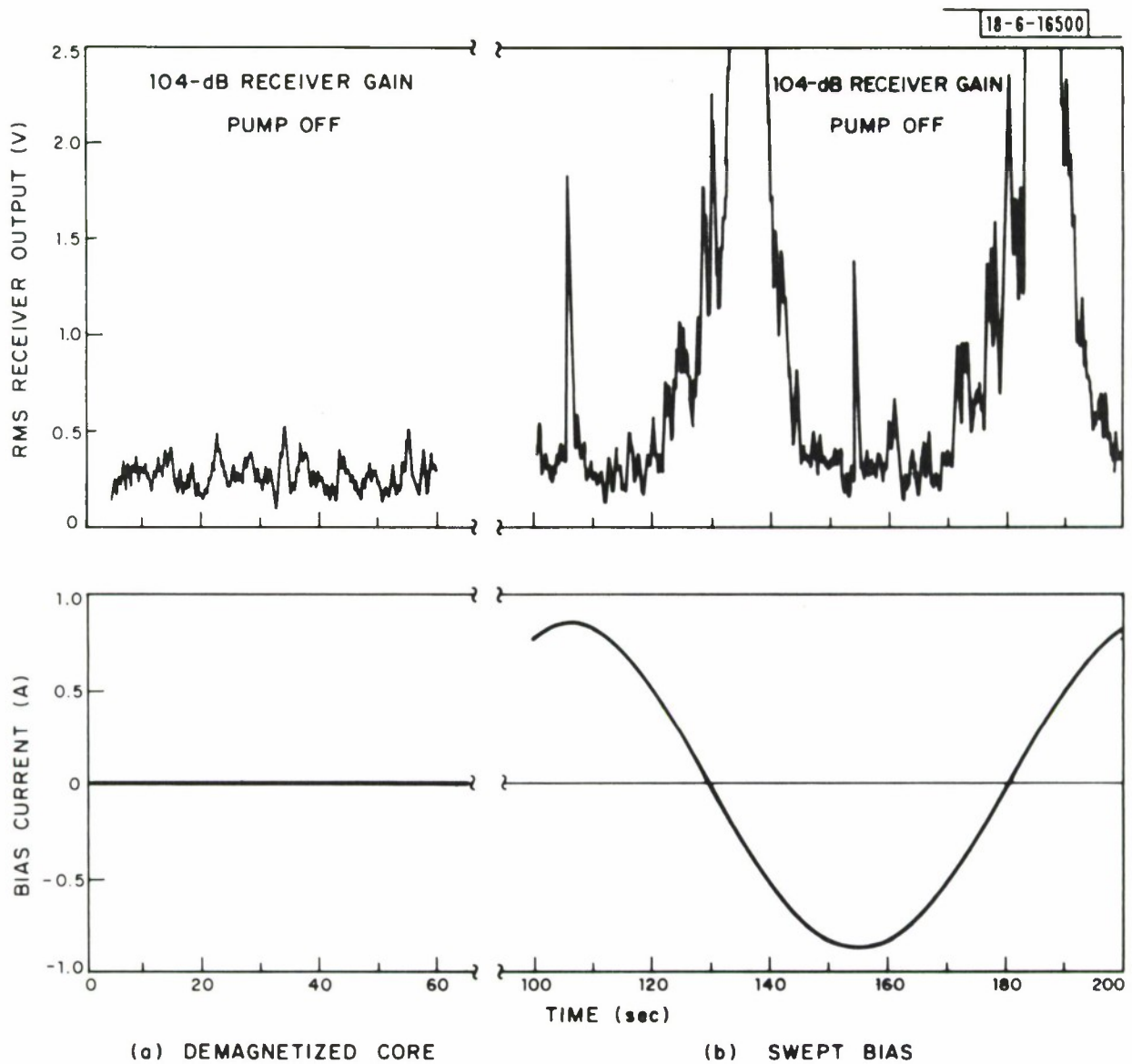


Fig. 3. Antenna noise measured in the water-flow tunnel with the pump off.
 (a) antenna core demagnetized, (b) magnetic bias swept cyclically at 0.01 Hz.

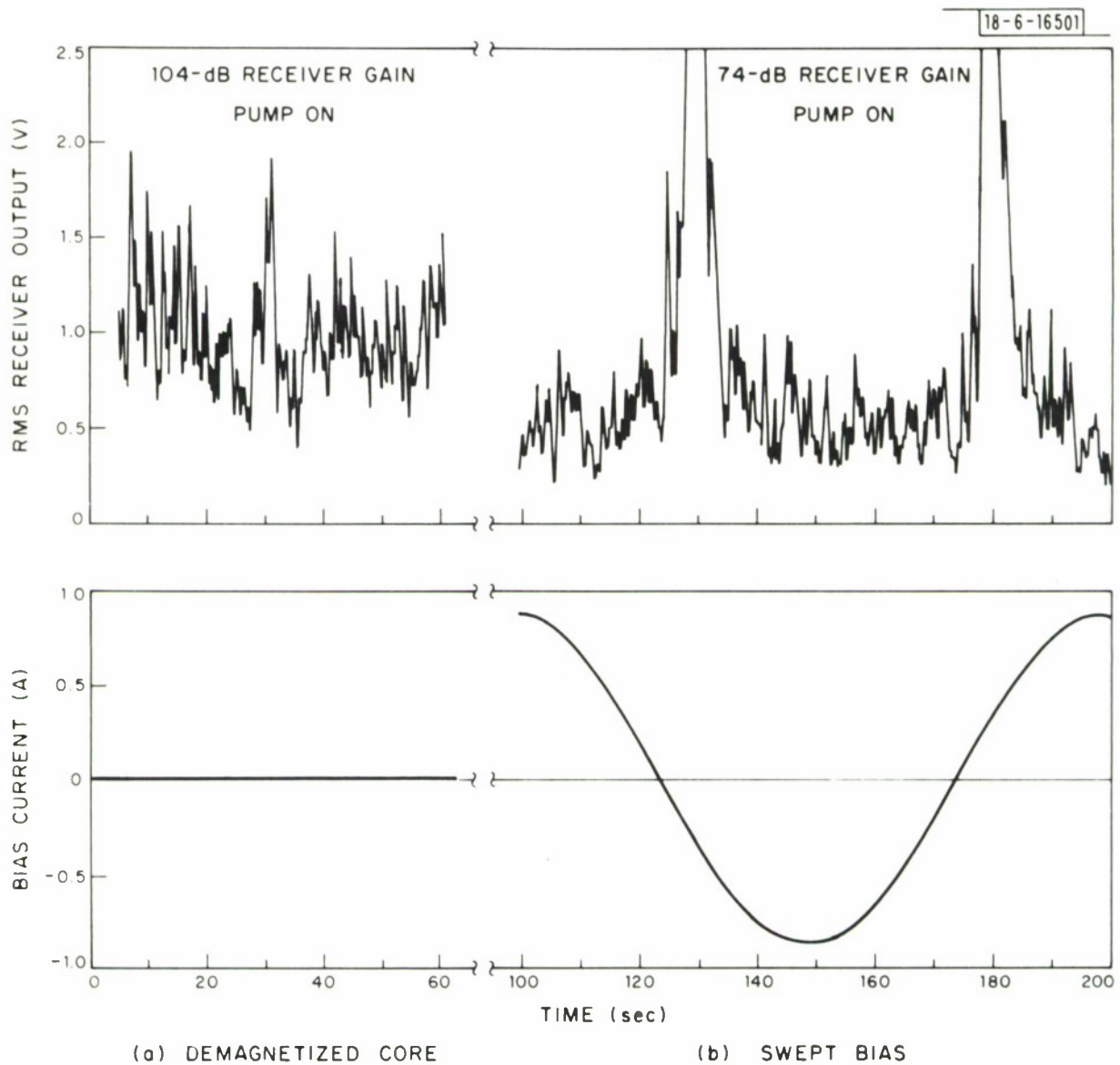


Fig. 4. Antenna noise measured in the water-flow tunnel with the pump on. (a) antenna core demagnetized, (b) magnetic bias swept cyclically at 0.01 Hz. Note reduced receiver gain for swept bias recording.

noise background of Fig. 3(b). Thus it requires both antenna vibration and a bias field for its generation. This is magnetostrictive noise.) The antenna used in these measurements was the square profile, 90 foot long antenna of the same internal design as the 1000 ft. long antenna successfully tested in March 1974 on the USS Pargo [6].

Incidentally, the impulsive transients in the receiver output shown, in Fig. 3(b), to coincide precisely with the peaks and troughs of the bias current, are spurious. They arise from a slight imperfection in the waveform of the function generator used to provide the bias sweep signal to the bias unit. The particular generator used for these measurements obtained its "sinusoidal" waveform output by a synthesis procedure. The imperfections were the result of an imperfect match between the up and down strokes of the waveform.

Figure 5 provides another example of the diagnostic noise-physics applications of the water-flow tunnel. Again the antenna under test was the 90-foot-long square-profile version of the "Pargo, 1974" antenna design [6]. The figure shows the antenna noise voltage spectral density at 25 Hz as a function of bias current as the bias current is swept from -0.85A to $+0.85\text{A}$. Only the region of the curve around the magnetostrictive minimum is shown. The curve confirms that the magnetostrictive effects observed on short specimens [7,8] in the laboratory and also in long antennas at sea are readily observed in the water-flow tunnel. The water flow was at maximum speed for these measurements. Each end of the antenna was restrained from transverse motion by means of four thin wire hooks extending from the tunnel wall.

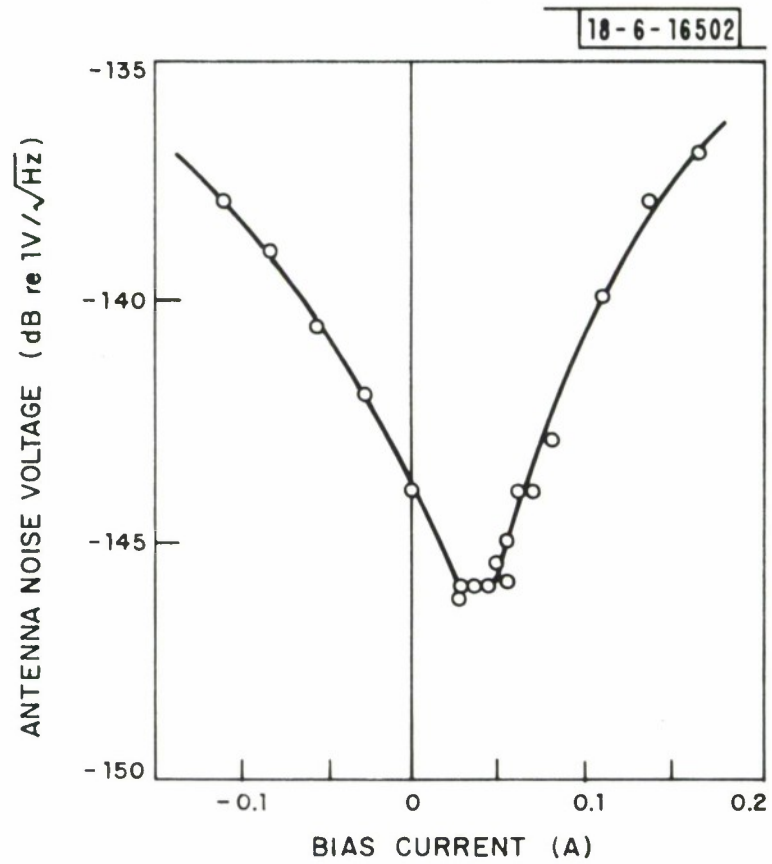


Fig. 5. Antenna noise voltage spectral density at 25 Hz as a function of bias current.

It has been believed for some time [9,3,10,11] that tapering the sensitivity profile of the antenna would reduce its motion-induced ENF. The first direct comparison of a tapered-profile antenna with a square profile one was made in the water-flow tunnel. Figure 6 shows the result of the comparison. The upper curve is the voltage noise spectrum of the unrestrained, demagnetized, square-profile antenna, and the lower one is the corresponding spectrum of the tapered-profile antenna. The upper curve has been reduced in level by 3 dB because the received signal level is also reduced by tapering the profile. Thus the difference between the two curves as drawn is the difference in their ENFs. The improvement gained by tapering is clear.

Theoretical considerations [3] indicate that the motion-induced ENF of an antenna is proportional to $\text{Av}\{|U(k_t)|^2\}/|U(0)|^2$, where $U(k)$ is the Fourier transform of the antenna's sensitivity profile, k_t is the wavenumber about which the transverse vibrational energy is concentrated for vibration at the frequency under consideration and $\text{Av}\{ \}$ denotes a local average around k_t . This quantity has been calculated from the measured sensitivity profiles of the square- and tapered-profile antennas tested in the tunnel. The result is shown, plotted as a function of frequency, in Fig. 7. For calculating k_t , the formula given in [3] was used, assuming that the tension was 150 lb and that the cable properties are those measured on a similar buoyant antenna cable and also given in [3].

By comparing Figs. 6 and 7, one sees that the 10 to 15 dB measured improvement (reduction) in motion-induced ENF obtained by going to a tapered profile is roughly in agreement with the improvement predicted theoretically.

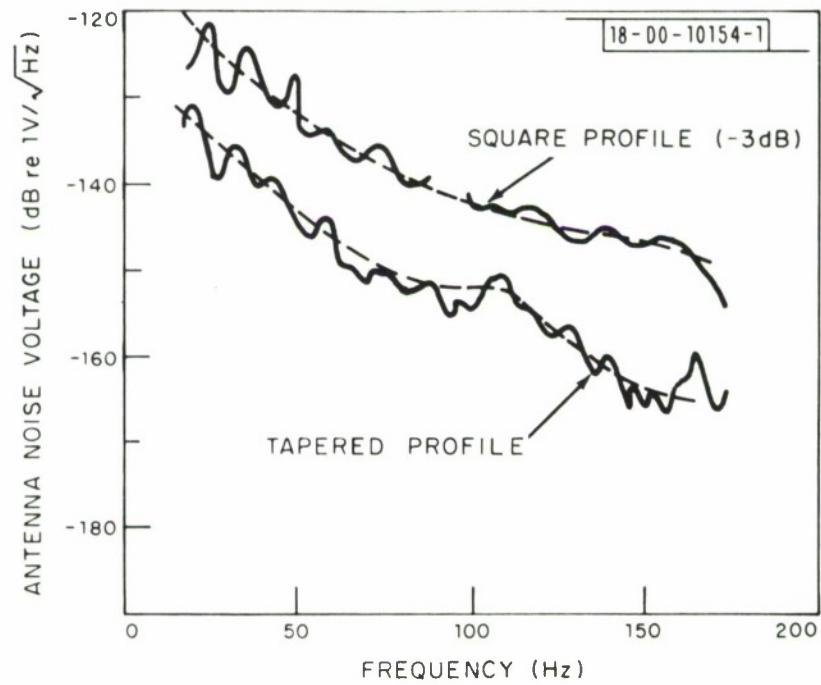


Fig. 6. The noise voltage spectra of square- and tapered-profile antennas measured in the water-flow tunnel in a demagnetized condition.

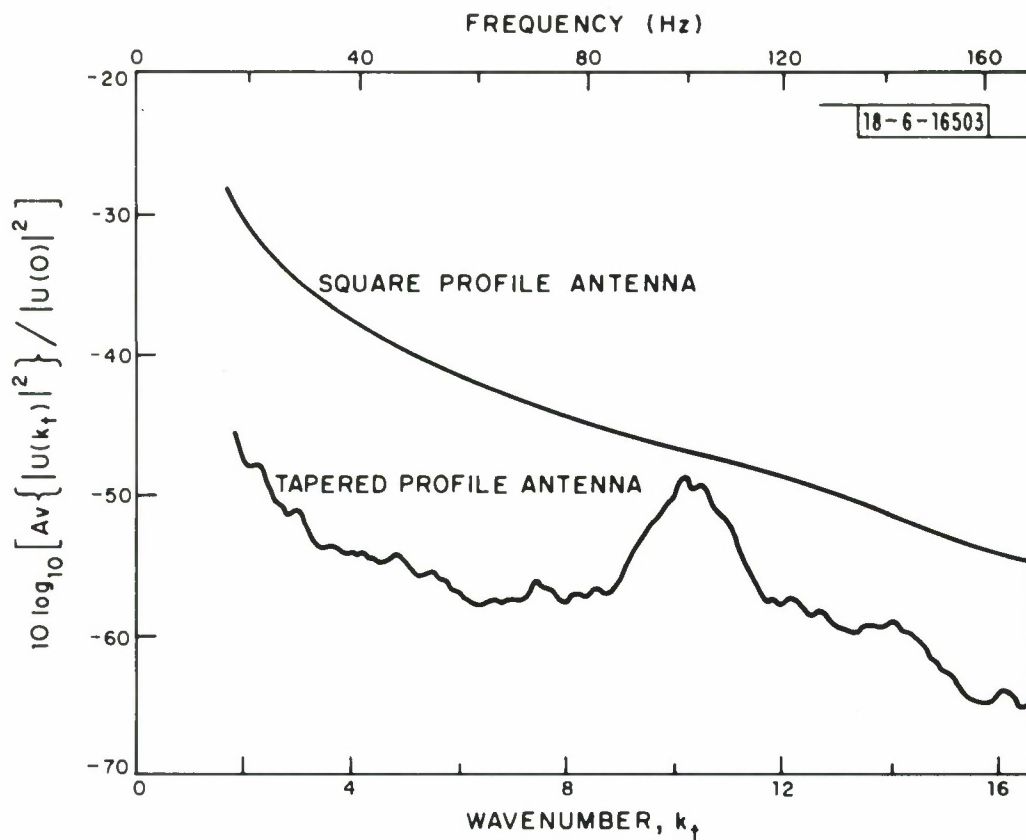


Fig. 7. The normalized and locally averaged Fourier transforms of the sensitivity profiles of the 90 ft. long tapered- and square-profile antennas.

The local maximum in ENF of the tapered-profile antenna at around 100 Hz is due to the step size used in the stepped-approximation to a smooth turns density variation. This local maximum is present in both measured and theoretical results.

Figure 8 shows the sensitivity profiles of the two antennas, measured using the technique described in [3].

In Section II, in the discussion of discrimination techniques, the procedure was described of restraining the ends of a square-profile antenna from vibrating in the transverse direction. By doing this, the dominant motion-induced noise of the short antenna is eliminated, hopefully to expose profile-roughness to measurement. Figure 9 shows the result of applying this technique to the 90 ft. long square-profile antenna in the water-flow tunnel. Except for a mysterious peak at around 80 Hz, the noise reduction is marked. It is believed that the peak is at the resonant frequency of the spring-mass system consisting of the four restraining hooks mass-loaded by cable at each end of the antenna.

These initial tests with the water-flow tunnel were very encouraging. They showed that all the known noise sources could be examined separately under realistic conditions but with laboratory-like convenience. The next important question was whether the tunnel could be used to obtain quantitative performance data of sufficient accuracy.

It would appear from Fig. 9 that the answer to this question is "Yes". For example, at 45 Hz the noise voltage generated by the unrestrained antenna is about $-127 \text{ dB relV}/\sqrt{\text{Hz}}$, which is an ENF of $-129 \text{ dB relV/m}/\sqrt{\text{Hz}}$, since the

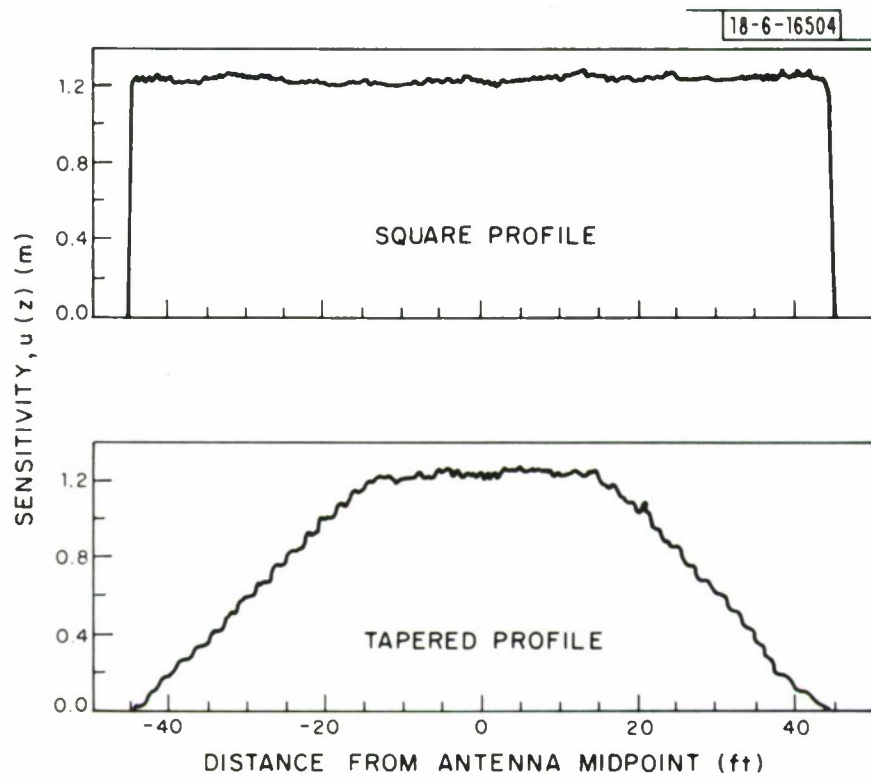


Fig. 8. The sensitivity profiles of the two antennas.

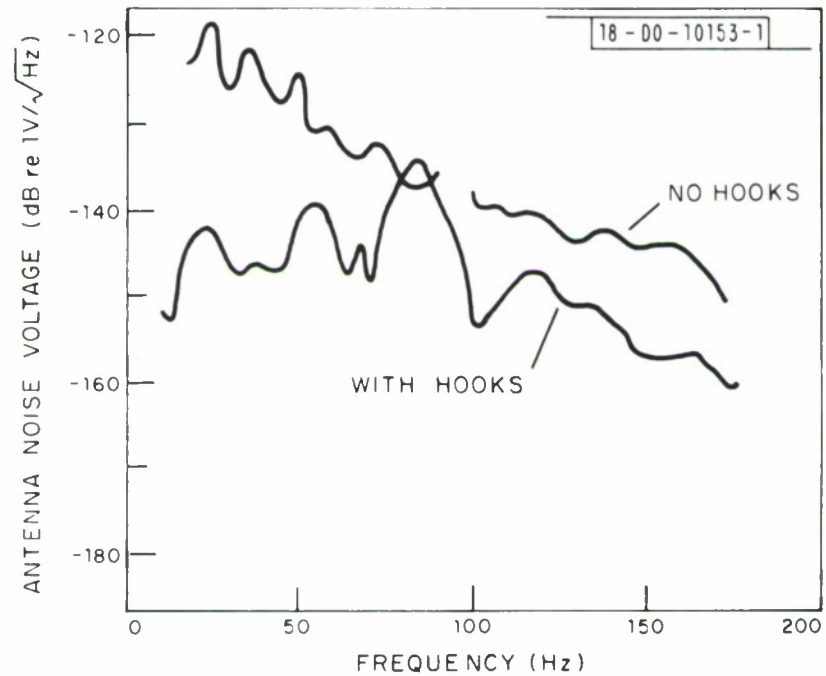


Fig. 9. The noise spectra of the square-profile antenna both with end restraint and without it. A demonstration of "end-effect".

antenna's effective length is 1.27m or 2.1 dB re.1m. But the mean-square end-effect motion-induced ENF is inversely proportional to the square of the antenna length. Thus a 1000 foot long antenna would have an end-effect motion-induced ENF of -150 dB re 1V/m/ $\sqrt{\text{Hz}}$ if its vibration along its whole length were statistically of the same amplitude as that of the antenna in the water-flow tunnel. But behind a submarine at 12 knots, a square-profile antenna generates [3] an end-effect motion-induced ENF of -173 dB re 1V/m/ $\sqrt{\text{Hz}}$. Thus the water-flow tunnel gives the cable 23 dB more transverse mechanical vibration than does a submarine tow at 12 knots.

This vibration amplitude scaling factor can now be used to scale the noise spectrum made with restraints and obtain an estimate for the profile-roughness ENF of a full-length antenna. From Fig. 9, the noise voltage at 45 Hz of the antenna under restraint is about -147 dB re 1V/ $\sqrt{\text{Hz}}$, so the ENF is -149 dB re 1V/m/ $\sqrt{\text{Hz}}$. But mean-square profile-roughness ENF is inversely proportional to length, so for a 1000-foot-long antenna, the ENF would be -160 dB re 1V/m/ $\sqrt{\text{Hz}}$. Since the excitation in the tunnel is 23 dB greater than behind a submarine, this implies finally, that behind a submarine at 12 knots, the profile-roughness ENF of a full-length antenna of the design tested in the tunnel would be -183 dB re 1V/m/ $\sqrt{\text{Hz}}$. This is gratifyingly close to the measured [6] profile-roughness ENF behind a submarine of -181 dB re 1V/m/ $\sqrt{\text{Hz}}$.

There is clearly a large measure of luck in the closeness of this result. If the comparison had been made at other frequencies, the noise estimates would have been as irregular as the lower curve in Fig. 9. A fair comment

would be that the estimate is accurate to within a few decibels.

However, since the scaling laws are based on the assumption that the cable vibration is statistically uniform along the length of the antenna, this conclusion depends on the validity of the uniformity assumption. The uniformity question is one of the considerations of the next section.

IV. Measurements of Vibration and Pressure

A buoyant cable instrumented with strain gages had already been built and used to measure the vibration (longitudinal and transverse) of a cable under tow from a submarine [2,12]. This same cable was used to measure antenna cable vibration in the water-flow tunnel. The vibration was measured at three different positions along the tunnel by moving the whole cable axially to bring the strain-gage pair into each new position. The results are shown in Fig. 10. For comparison, spectra taken at 12 knots at sea with the same cable are also shown.

The two prominent features of these curves are first, the extent to which the tunnel vibration spectra exceed the at-sea spectra--a result predicted by the antenna measurements--and, second, the amount by which the tunnel spectra differ from one another. The first of these features is unremarkable and expected. It has been discussed in earlier sections. The second feature, however, indicates a substantial non-uniformity in vibration level along the length of the test section. It detracts from the ability of the flow-tunnel to predict antenna performance accurately.

Since the vibration at station 1 (the upstream end of the test section) is some 10 dB larger than it is at station 5 (the downstream end), the motion-

induced noise of the square profile antenna is generated mainly at station 1. Thus the motion-induced noise voltage should be just 3 dB less than it would be were the vibration uniform and at the level existing at station 1.

Using the formulas and cable data of [3] and the station 1 curvature spectrum from Fig. 10, the motion-induced noise voltage for the antenna was computed. The resulting spectrum, reduced by 3 dB for the reason given in the last paragraph, is presented in Fig. 11 together with the measured spectrum from Fig. 9. The agreement is not bad, showing that the quest for quantitative precision is not unreasonable.

The measured non-uniformity in cable vibration might be caused by a non-uniform turbulence over the length of the test section. It might also be caused by mechanical excitation occurring outside the test section. The measured vibration would then arise by propagation of the disturbance along the cable itself into the test section.

To investigate this point further, flush-mounted hydrophones were placed at the inside wall of the tunnel at stations 1, 3 and 5. The resulting fluctuating wall pressure spectra are shown in Fig. 12. Since these three spectra are within 2 or 3 dB of one another over the whole frequency range of interest, it is clear that the much larger difference between the cable vibration measurements at the three stations (Fig. 10) is due to some disturbance propagating into the test section along the cable.

Incidentally, to measure these pressure fluctuation spectra, it was necessary to mount two matched hydrophones diametrically opposite one another

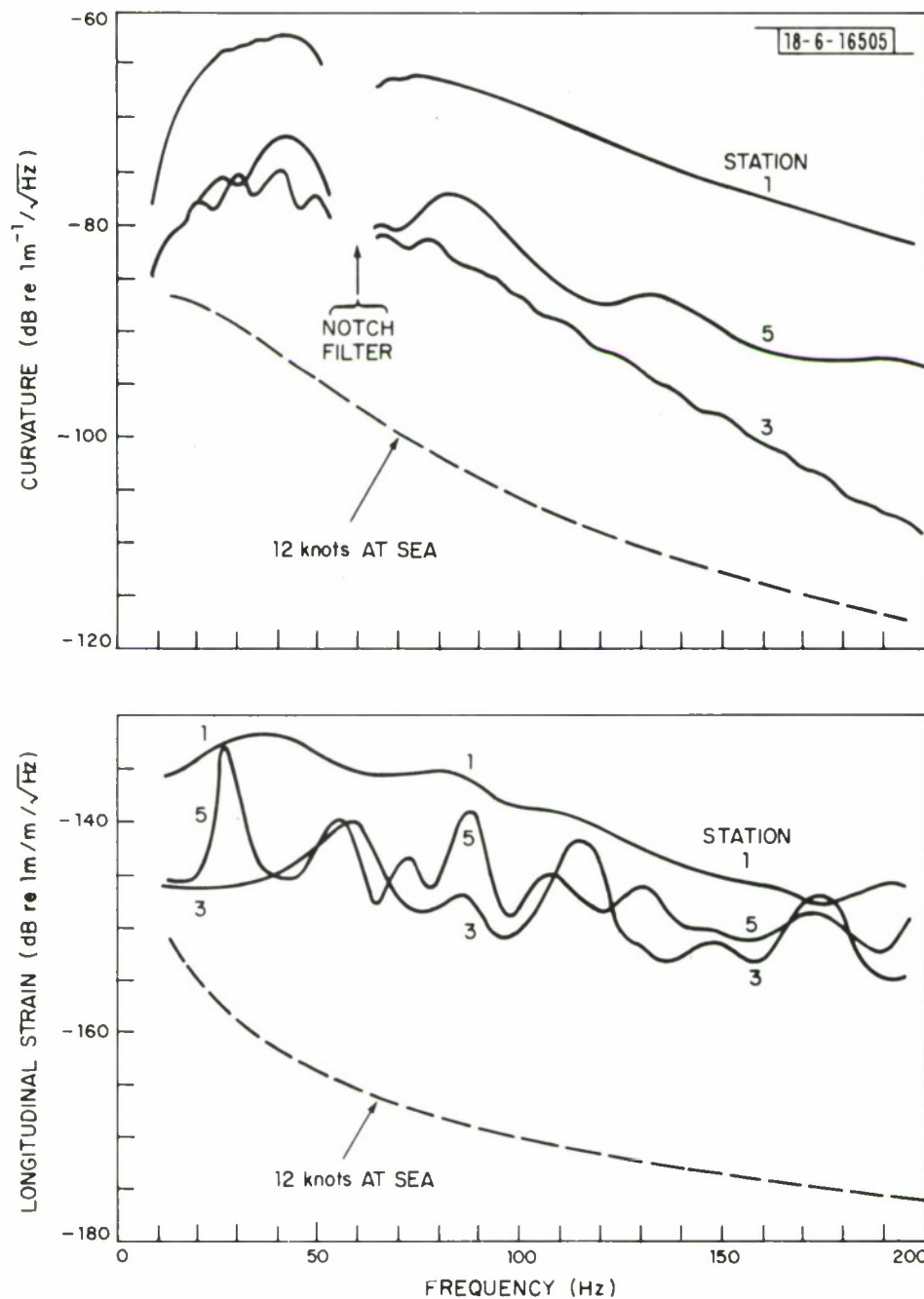


Fig. 10. The spectra of cable curvature and longitudinal strain measured in the water-flow tunnel at three stations (see Fig. 1). For comparison, the same spectra measured at 12 knots at sea are included.

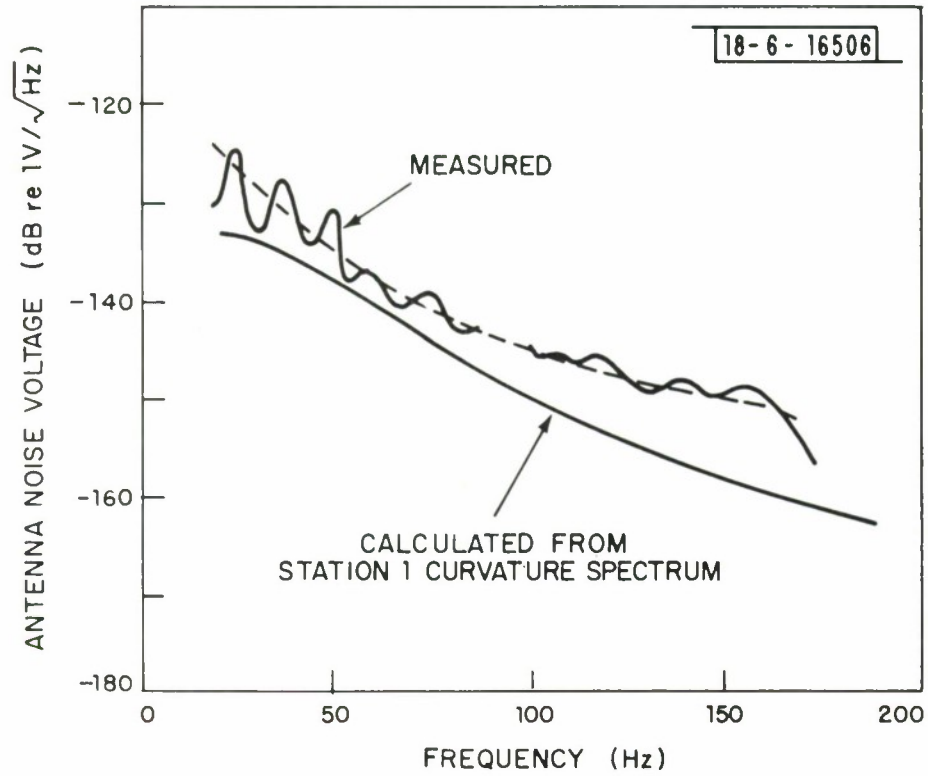


Fig. 11. The measured motion-induced noise of the square-profile antenna compared with that calculated from the cable curvature measurements.

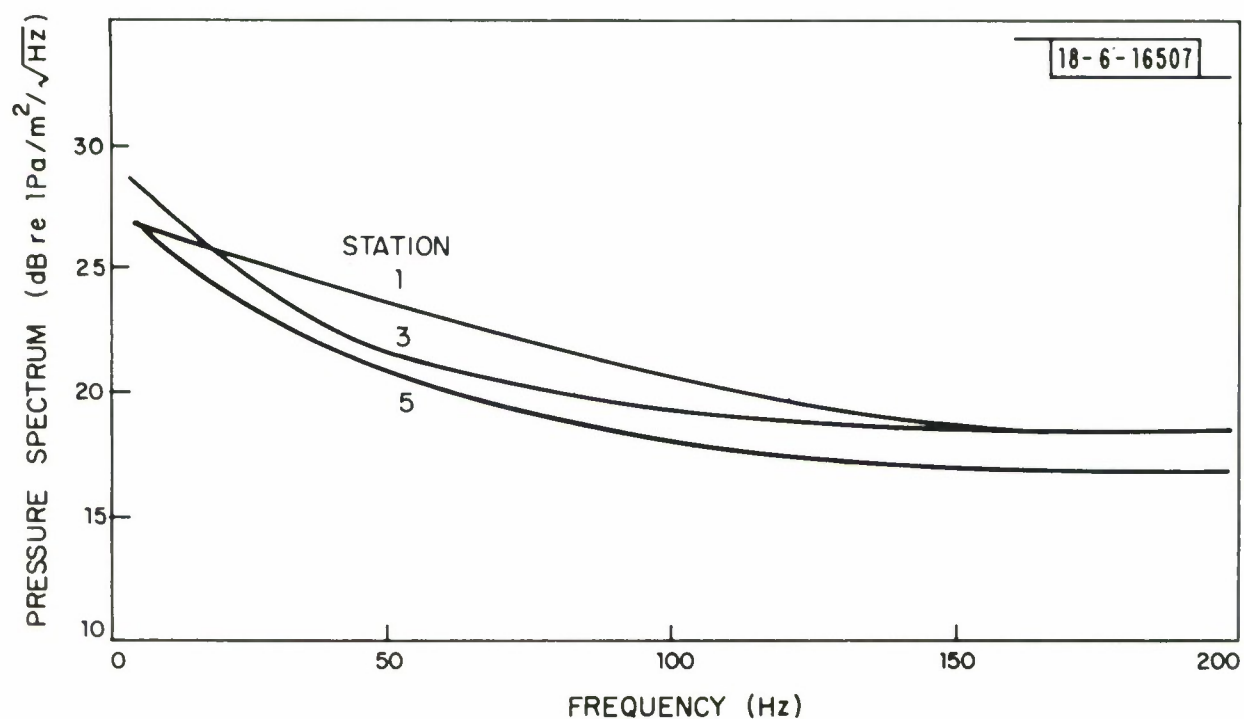


Fig. 12. Wall pressure fluctuation spectra measured at each end of the test section (stations 1 and 5) and at the mid-point (station 3).

across the tunnel and use the difference between their output voltages as the pressure data. A single hydrophone measures both the turbulent pressure fluctuations and the acoustic pressure variations in the water. The latter, generated mainly by the pump, are essentially in-phase and of constant amplitude over any particular tunnel cross-section. Thus they do not excite the cable into motion but they are present in each hydrophone output. The technique of taking the difference in pressure between two circumferentially spaced hydrophones rejects the common mode acoustic pressure signals but retains the uncorrelated turbulent pressure fluctuation signals.

The measured turbulent pressure fluctuation spectra are in good agreement with those reported by other workers. For example, at 45 Hz and at station 3, the nondimensional turbulent pressure fluctuation spectral level $2 \overline{p^2} / (\rho \overline{u}^3 d) / \text{B.W.}$ is -49.8 dB. $[\overline{p^2} / \text{B.W.}$ is, from Fig. 12, 22 dB re. 1Pa/ $\sqrt{\text{Hz}}$, ρ is 10^3 kg/m^3 (1g/c.c), d is 0.152m (6 inches) and \overline{u} is 5.86 m/s (11.4 knots)]. But the measurements of turbulent pressure fluctuation spectra reported in the literature result in nondimensional spectral levels lying around -53 dB [13].

From these measurements of turbulent pressure fluctuations and of cable vibration, it was inferred that the cable was being mechanically excited upstream of the test section at the exit from the stilling chamber. The judgment was that the square section spokes of the turbulence inducing sprocket and the blunt end of the tubular cable guide were causing an excessive amount of turbulent eddying (See Fig. 7 of Ref. [1]). These strong eddies were then impinging directly on the cable as it emerged from the cable guide.

To test this conjecture, the sprocket spokes were reworked to make them

streamlined, a faired hub was added on the upstream side of the sprocket and a conical fairing was fastened to the end of the cable guide. In addition, the whole aperture at the sprocket was covered with a perforated screen.

Measurements of the cable vibration and of the turbulent pressure fluctuations made after these modifications are shown in Figs. 13 and 14. They show that much of the inlet end problem has been eliminated in that the turbulent pressure fluctuation spectra at the three stations are essentially identical, the transverse cable vibration at the first four stations is clearly uniform and the levels of both the pressure fluctuations and the cable vibration are less than they were before the inlet modifications. The pressure fluctuation level now agrees very closely with the levels reported in the literature [13].

There remains a growing deviation from uniformity in transverse vibration at the inlet end at higher frequencies. There also exists a higher level at station 5 over the whole frequency range. That both of these end problems are amenable to further improvement was demonstrated by first providing a faired, smaller diameter extension to the cable guide tube at the inlet end, to shield the cable from the remaining eddies coming off the modified sprocket. It was found that there was further reduction in the transverse vibration level at station 1, as Fig. 15 shows. The level at other stations was essentially unchanged.

The outlet end problem was shown to be due to cable excitation by eddies generated at tunnel wall irregularities. A crude fairing over the six-inch access port at the outlet end was rotated by 90° by simply rotating the port

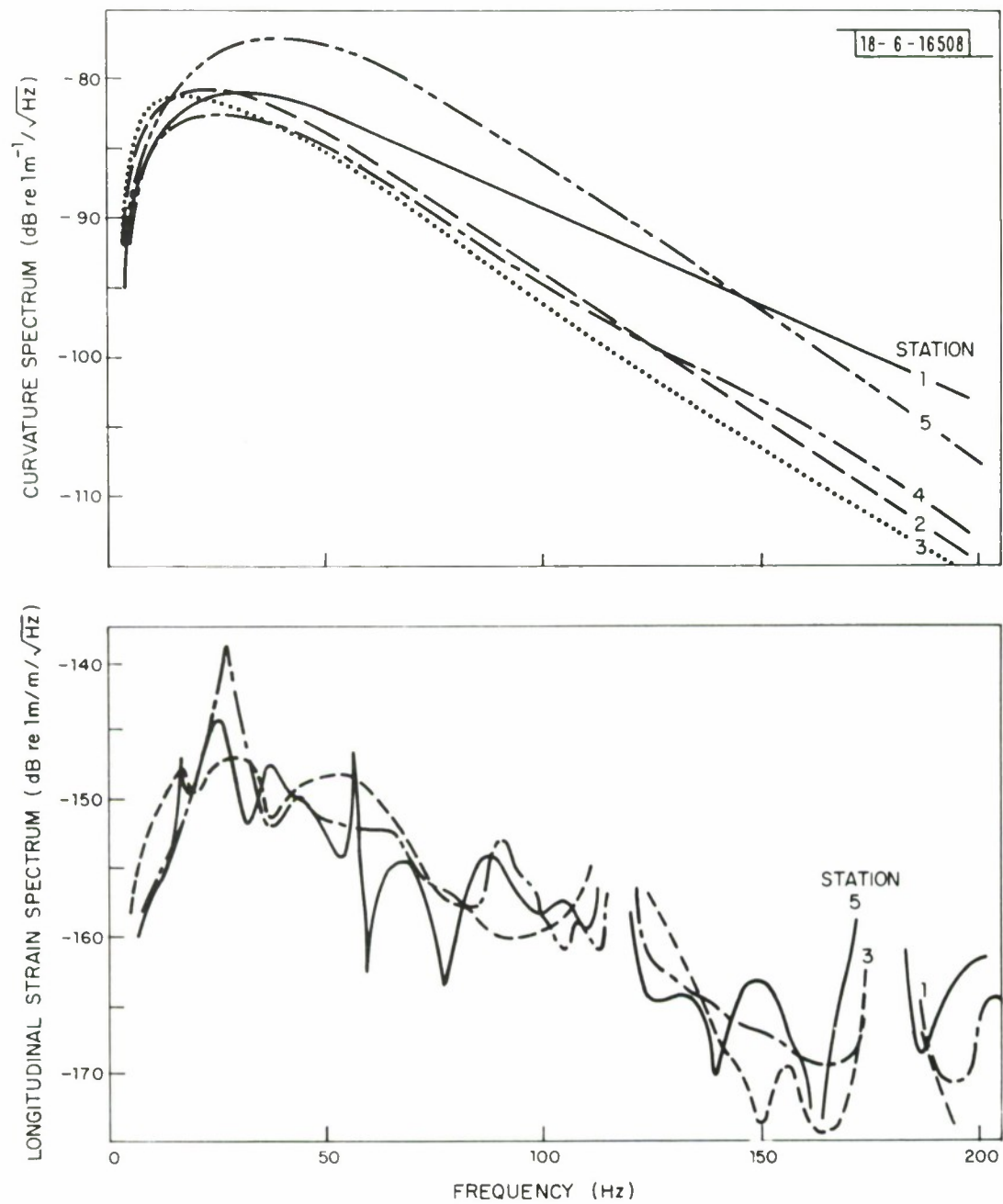


Fig. 13. Cable vibration spectra (curvature spectra and longitudinal strain spectra) measured at several stations after inlet modifications.

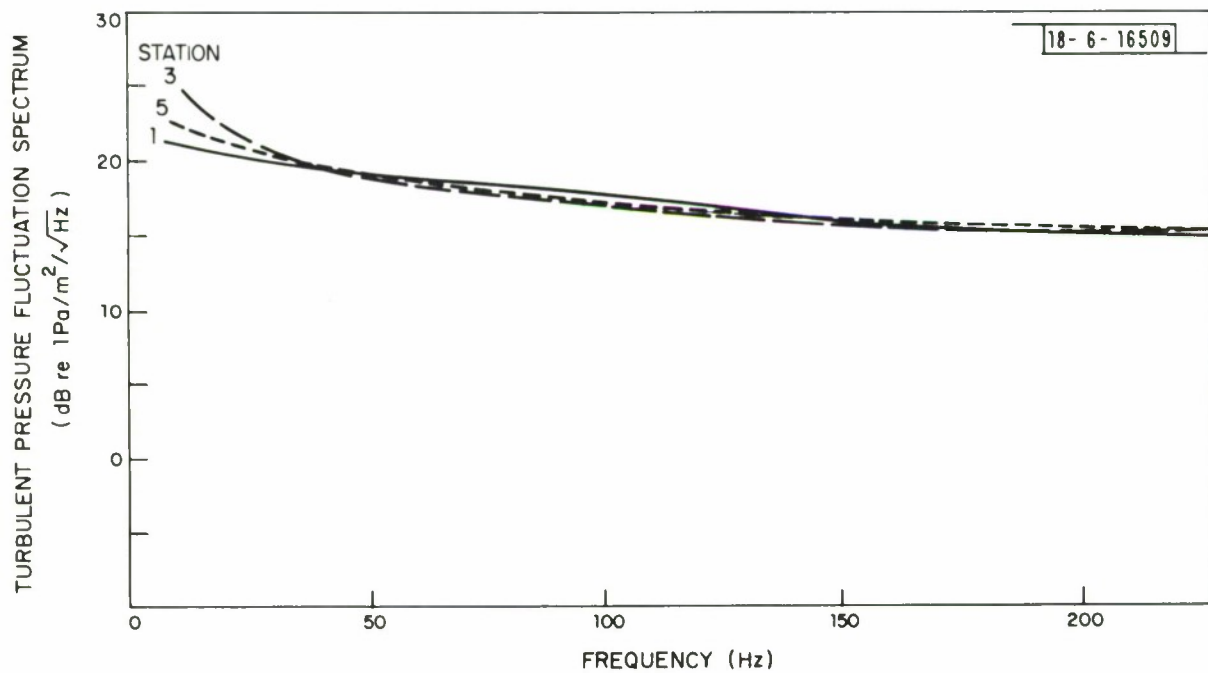


Fig. 14. Wall pressure fluctuation spectra measured at three stations after inlet modifications.

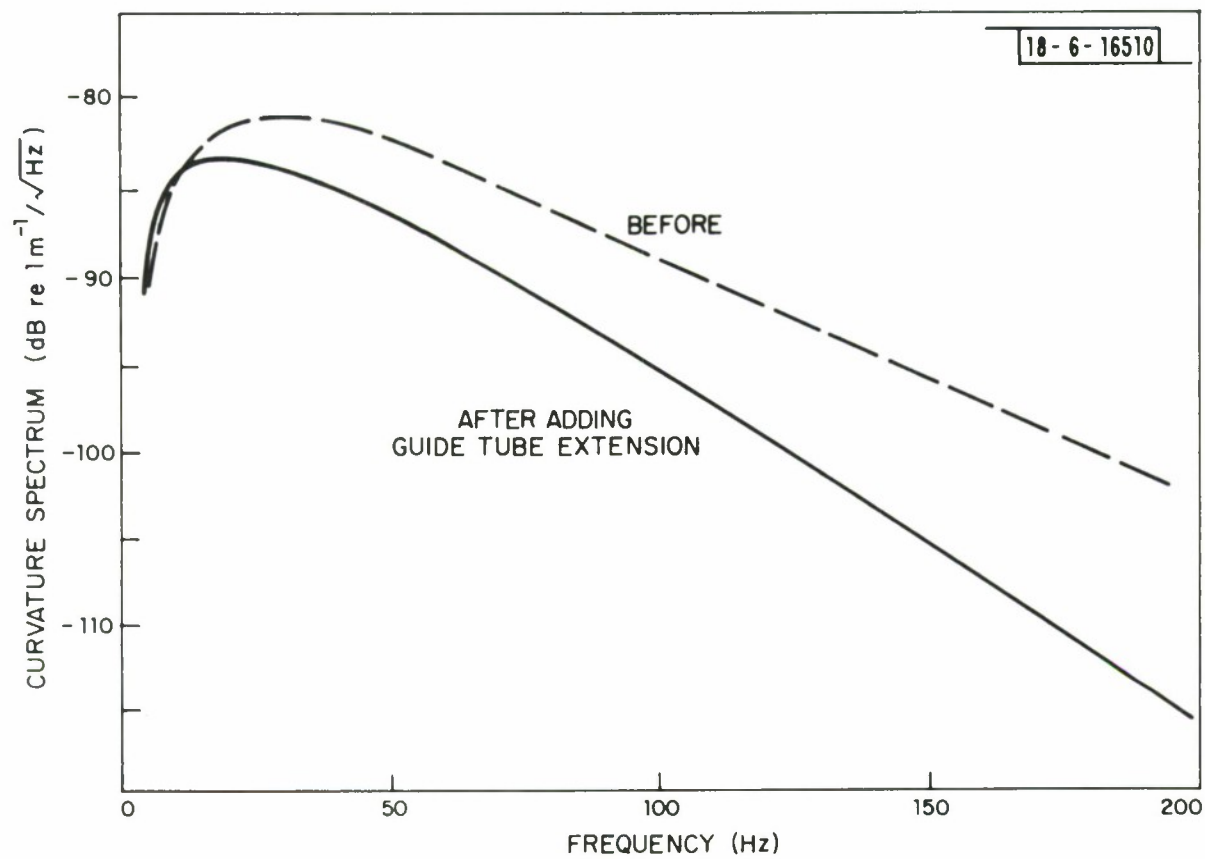


Fig. 15. Cable curvature spectra at station 1 before and after adding the guide tube extension.

cover. This increased the irregularity of the wall, because the fairing was shaped to conform to the wall curvature. The effect was to increase the transverse cable vibration at station 5 by some 5 dB over the whole frequency range.

The physical configuration of the outlet end made it difficult to provide an extension to the outlet end cable guide tube, but it would be expected that the combination of a longer guide tube and smoother tunnel walls should eliminate the outlet end non-uniformities.

Turning to the longitudinal strain spectra of the cable, one sees, by comparing Figs. 10 and 13, that the general level went down after the inlet end modifications and that on average more uniformity was gained from station to station. However, the jagged nature of the spectra was, if anything, aggravated. It is characteristic of the many longitudinal strain spectra, taken before and after modification, that they are both jagged and non-repeatable in detail. The non-repeatability entails the failure to reproduce the same spectrum if the cable has been moved between each measurement, even though the gage pair is brought back to the same position. If the cable remains in the same position between successive spectral measurements, and if the mechanical end terminations are not changed in any way, then repeatable spectra are obtained. The graph displayed in Fig. 5 could not have been obtained were it otherwise.

The jagged nature of the longitudinal strain spectra is due to the low attenuation of longitudinal strain waves in the cable over the length of the tunnel. In contrast to the case of transverse vibration, therefore, the longi-

tudinal vibration exhibits a line spectral response, with peaks in vibration level occurring at the frequencies at which the cable length is an integral number of half wavelengths. The situation is complicated further by the fact that the nodes and anti-nodes of the vibration lie at locations, with respect to a particular strain gage pair, which change as the frequency changes from one resonant frequency to the next. And finally, the nature of the end terminations is not fixed. Depending on the tightness of the water seal gland, the effective termination point could be anywhere between the gland and the actual cable anchor. The vibrational absorbing properties of the termination are also affected by the gland adjustment. This means that the resonant peaks in cable vibration can change in both frequency and sharpness.

It is clear that some redesign is necessary to obtain a longitudinal vibration of the cable both uniform and repeatable enough for performance prediction purposes.

An attempt was made to remeasure the antenna noise spectra after the inlet modifications were made to the system. However, it was found impossible to obtain a repeatable spectrum. Each demagnetization was followed by a spectrum of a new shape, although this was repeatable provided no demagnetization occurred between it and the repeat measurement. The relative level of the curvature to the longitudinal strain was much the same after the inlet modifications as it had been before, and so the discrimination problem should have been no more difficult. The only explanation seems to be that the process of threading the antenna through the tunnel and winding it back onto its reel, repeated many times, had changed the properties of the ant-

enna's magnetic core by, for example, working it mechanically in the presence of the earth's field and thereby establishing an irregular remanent magnetization. This question needs to be examined more thoroughly for it has possible implications about the useful life of an operational antenna.

V. Improvements

There are certain inlet and outlet modifications that should be made to improve the uniformity of the cable vibration over the whole test section length. These should involve a permanent faired extension to the cable guide tubes at both inlet and outlet ends, and establishing a smooth tunnel wall wherever the cable is unprotected by a guide tube. In addition, some thought should be given to providing improved and stable cable terminations at each end. Ideally, the terminations should be as mechanically absorptive as possible. Then the strong longitudinal mode resonances would be damped, giving a smoother longitudinal vibration spectrum which is also more uniform along the test section. A further benefit would be a reduction in level of the resulting magnetostrictive noise without reducing the motion-induced noise. This would help in the difficult problem of discrimination.

VI. Conclusions

The water-flow tunnel can rapidly provide test data on ELF submarine-towed antennas attainable otherwise only slowly on a submarine. Its thick aluminum shielding creates within the tunnel the electromagnetically quiet environment of the ocean at depths of operational interest; the fully-developed turbulence within the tunnel excites the antenna cable essentially uniformly along its length, as does the self-excited turbulent boundary layer of a

cable under tow; and, using a bias winding on the antenna, the axial magnetic bias field can be varied to simulate heading changes.

The tunnel has been used to reproduce, in specially constructed test antennas, all the motion-related noises known to afflict the towed ELF loop antenna. Good agreement has been obtained with the theory of antenna noise generation and also with measurements made at sea on full-length antennas. In particular, the end effect for motion-induced noise in square-profile antennas has been demonstrated, and the predicted reduction in motion-induced noise obtainable by tapering the profile has been corroborated by direct measurement.

No new noise source has been uncovered by the work carried out so far in the water-flow tunnel, with the exception of an apparent "aging effect". This is, the magnetostrictive noise of the antenna, after demagnetization, appeared to increase with the life of the antenna. More work is needed to confirm this, however.

Acknowledgements

Credit is due to L. F. Mullaney, for his resourceful and able site management; to R. T. Hall, for the scale model shielding measurements; and especially to S. E. Forman, for his role as designer and builder of the tunnel and for his continuing valuable assistance, both technical and manual, in testing it.

APPENDIX A

ELECTRICAL EFFECT OF TUNNEL WALL

When an alternating current passes through the antenna winding, an electric field external to the winding is generated. If the antenna is enclosed by the tunnel, this field induces currents in the tunnel wall, which in turn generate a field of their own. The input impedance of the antenna is given by the net effect of the two fields, together with the resistance of the antenna's winding.

Thus it can be shown that the antenna impedance per unit length Z is given by

$$Z = R_o + j\omega L_o \left\{ 1 - \frac{A_e/A_o}{1 + A_e/A_o - A/A_o + (1-j)\delta/b} \right\}. \quad (A1)$$

Here R_o is the antenna's winding resistance per unit length, L_o is the antenna inductance per unit length, A_e is the effective core area (the core sensitivity ν in Wb/A/m divided by the permeability of free space μ_o), A_o is the cross sectional area of the tunnel, A is the actual core area (the area enclosed by the antenna winding), δ is the skin depth in the material of the tunnel wall and b is the tunnel radius. Thus provided $A_e/A_o \ll 1$, the tunnel has negligible effect on the magnitude of the antenna impedance.

A typical core sensitivity might be 1.5 nWb/A/m, so that $A_e = 1.19 \times 10^{-3} \text{ m}^2$. Thus, with a tunnel radius of 3 inches, $A_e/A_o = 0.066$. This means, according to (A1), that the effect of the tunnel is to modify the antenna impedance by at most 7%.

The effect on the antenna resistance needs to be examined separately, for if the thermal noise level of the antenna is extremely low, it is possible that its resistance can be profoundly modified without much change to the magnitude of the impedance.

From (A1), by direct manipulation, it can be shown that

$$\frac{\Delta R}{R_o} = \frac{A_e \delta / (A_o b)}{[1 + (A_e - A) / A_o + \delta / b]^2 + \delta^2 / b^2} \frac{\omega L_o}{R_o} \quad (A2)$$

where ΔR is the change in antenna resistance per unit length attributable to the presence of the tunnel. Whether this change is significant depends upon how small R_o is to begin with. Since experience has shown that it is difficult to make a 300m long submarine towed loop antenna with a thermal equivalent noise field (ENF) as low as the total ENF at 12 knots of the 300m electrode-pair, a realistic lower bound on R_o can be obtained by assuming that the loop antenna's thermal ENF just equals it. That is [3],

$$\frac{4k_b T_k R_o 2\ell_e}{\ell_e^2} = 10^{-20.5} \quad (A3)$$

where k_b is Boltzmann's constant, T_k is the temperature in °K and ℓ_e is the effective length of the antenna, given by

$$\ell_e = \sqrt{2} A_e N 2\ell / \delta_o, \quad (A4)$$

where N is the turns density of the signal winding and δ_o is the skin depth in the ocean.

Since L_o also appears in (A2), the expression for it is also needed. It is

$$L_o = \mu_o N^2 A_e \quad (A5)$$

By combining (A3), (A4) and (A5), one finds

$$\frac{\omega L_o}{R_o} = \frac{\omega \mu_o k_b T_k \delta_o^2}{A_e \ell} 10^{20.5},$$

so that, from (A2)

$$\frac{\Delta R}{R_o} < \frac{A_e \delta}{A_o b} \cdot \frac{\omega L_o}{R_o} = \frac{\omega \mu_o k_b T_k \delta_o^2 \delta}{A_o \ell b} 10^{20.5}.$$

With aluminum having a conductivity of 3.57×10^7 S/m as the tunnel shielding material and sea water with a conductivity of 4 S/m as the operating medium, the skin depths δ and δ_o work out at 45 Hz to be 0.0126m and 37.5m, respectively. Then, with $\ell = 150$ m and $b = 0.0762$ (3"), the right side is numerically 0.0395. That is

$$\frac{\Delta R}{R_o} < 0.0395,$$

so the change in R_o due to the presence of the tunnel is less than 4% at 45 Hz.

APPENDIX B

MODEL SHIELDING MEASUREMENTS

To insure that the shielding of the tunnel was adequate, shielding measurements were conducted before construction using specially prepared tunnel sections of about one-sixteenth scale. A small search coil was used to sample an 8 kHz magnetic field before and after the tunnel section was placed around the coil. The field was applied by means of a 1 foot diameter multiple turn loop concentric with the search coil. The full-scale frequency is 31.25 Hz.

Figure B-1 shows the shielding effect of a simple thick-walled aluminum tube as a function of the search coil axial position. It shows that the expected shielding effectiveness is attained within less than two tube diameters from the end and that the shielding is equally good for both longitudinal and transverse fields.

Figure B-2 shows the shielding effect in the vicinity of a simple butt joint between two thick-walled tubes. The near transparency to transverse fields at the joint location is clearly shown.

Figure B-3 shows the shielding effect in the vicinity of a special overlapped joint. For this particular series of measurements, the tubes were precise one-sixteenth scale models of the candidate design of tunnel sections. On the basis of these measurements, which show a marked improvement in the shielding of transverse fields, it was decided to adopt this joint geometry for the full-scale tunnel.

18-6-16511

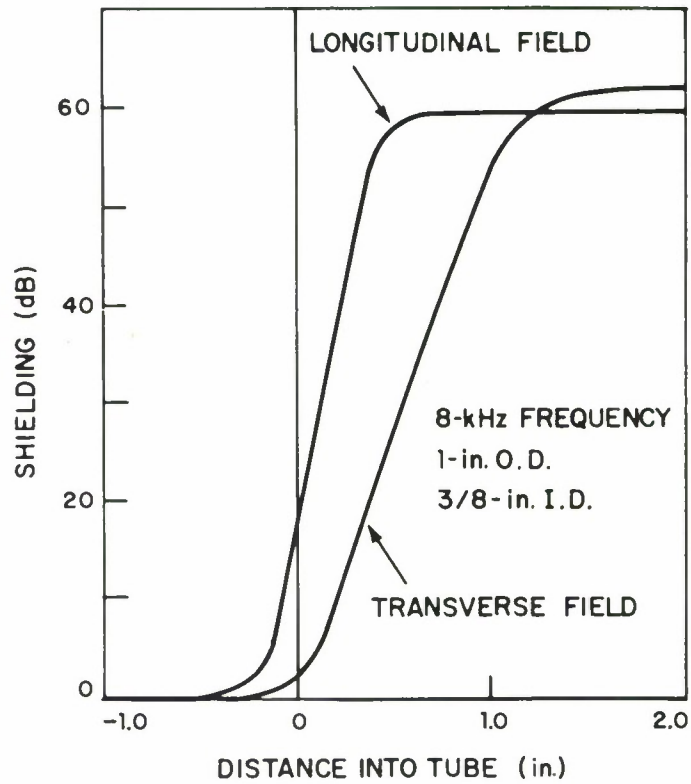


Fig. B-1. The shielding effectiveness of a thick-walled aluminum tube in the vicinity of the tube end.

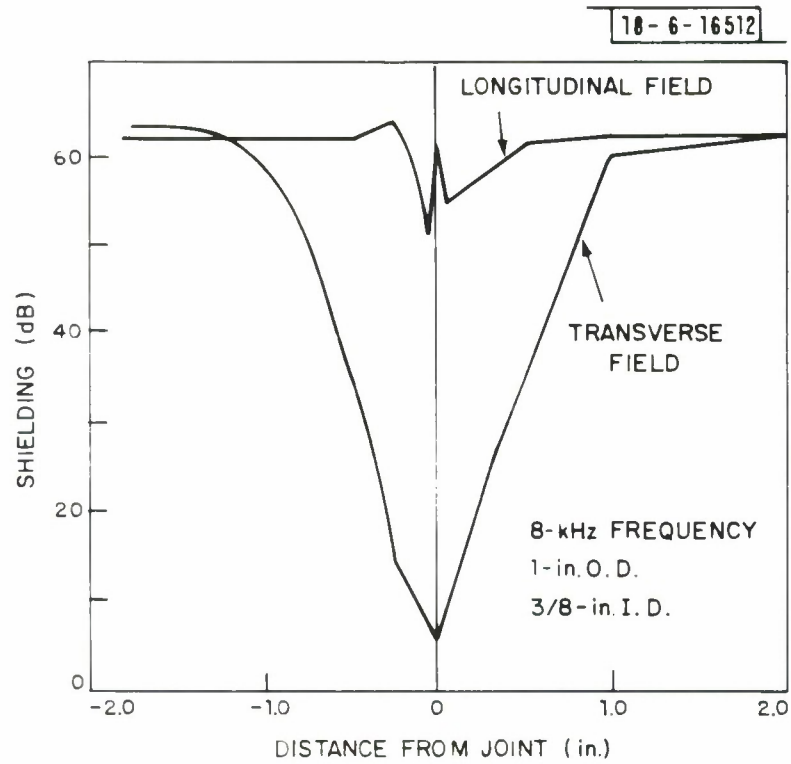


Fig. B-2. The shielding effectiveness of a thick-walled aluminum tube in the vicinity of a simple butt joint.

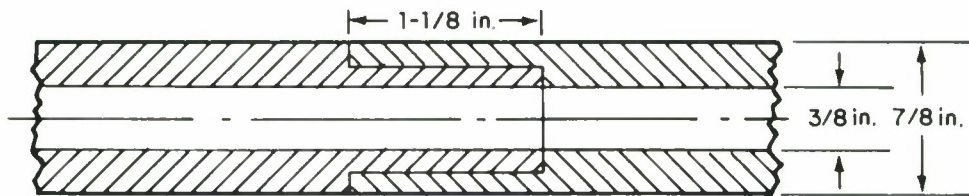
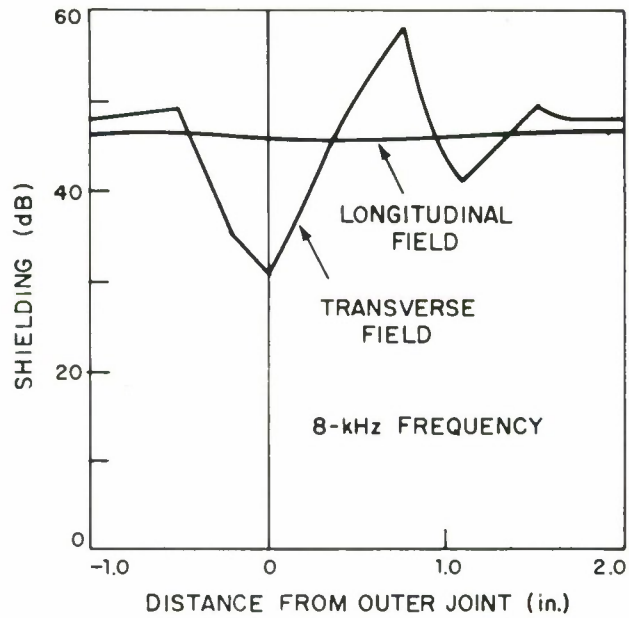


Fig. B-3. The shielding effectiveness of a thick-walled aluminum tube in the vicinity of an overlapped joint.

References

1. S. E. Forman, "ELF Antenna Flow Test Facility," Technical Note 1974-27, Lincoln Laboratory, M.I.T. (23 April 1974), DDC AD-778832/6.
2. M. L. Burrows, "Strain-Gage Vibration Measurements on a Submarine-Towed Antenna Cable," Technical Note 1975-22, Lincoln Laboratory, M.I.T. (27 May 1975), in press.
3. M. L. Burrows, "On the Design of a Towed ELF H-Field Antenna," Technical Note 1972-34, Lincoln Laboratory, M.I.T. (28 December 1972), pp. 67-73, DDC AD-754949.
4. M. L. Burrows, "Motion-Induced Noise in Electrode-Pair Extremely Low Frequency (ELF) Receiving Antennas," IEEE Commun. COM-22, 540-542 (1974), [Technical correction to paper in COM-22, 1154 (1974).]
5. M. L. Burrows, "Other Sources of Motion-Induced Noise in a Towed ELF H-Field Antenna," Technical Note 1973-21, Lincoln Laboratory, M.I.T. (25 May 1973), DDC AD-762936.
6. M. L. Burrows, "The Lincoln Submarine Towed ELF Loop Antenna," Technical Note 1975-24, Lincoln Laboratory, M.I.T. (27 May 1975), in press.
7. A. D. Cafaro, L. Dalsass and D. O'Brien, "Stress-Induced Noise in Magnetic-Cored H-Field Antennas," IEEE Commun. COM-22, 543-548 (1974).
8. M. L. Burrows, "Helically Wound Permalloy Tape Cores for ELF Antennas," Technical Note 1974-52, Lincoln Laboratory, M.I.T. (21 November 1974), DDC AD-A002316/8.
9. M. L. Burrows, "Motion-Induced Noise in Towed Flexible Sensors," Project Report NAC-15, Lincoln Laboratory, M.I.T. (24 March 1969).
10. R. L. Crane, "Motion-Induced Noise in Flexible Electrode-Pair and Loop Antennas," Technical Memorandum No. 1, RCA David Sarnoff Research Center, Princeton, New Jersey (July 1972).
11. A. Pelios, "Motion-Induced Noise in Trailed Antennas," Technical Memorandum No. 2, RCA David Sarnoff Research Center, Princeton, New Jersey (October 1972).
12. O. G. Nackoney, "Strain Gage Instrumentation of a Buoyant Cable," Technical Note 1972-18, Lincoln Laboratory, M.I.T. (30 March 1972), DDC AD-744825.

13. R. R. Walters and C. S. Wells, "Effect of Dilute Solutions of Drag-Reducing Additives on Wall Pressure Fluctuations," U. S. Navy Journal of Underwater Acoustics, 385-401 (April 1970).

OUTSIDE DISTRIBUTION LIST

Chief of Naval Operations Attn: Capt. W. Lynch (OP941P) The Pentagon Department of the Navy Washington, D.C. 20350	Mr. George Downs Strategic Systems, Electronic Sys. Gr. GTE Sylvania, 189 B Street Needham, Mass 02194
Chief of Naval Research (Code 418) Attn: Dr. T. P. Quinn 800 North Quincy St. Arlington, Va. 22217	Naval Electronic Systems Command Attn: PME-117-21A, Dr. B. Kruger Department of the Navy Washington, D.C. 20360
Computer Sciences Corp. Systems Division Attn: Mr. D. Blumberg 6565 Arlington Blvd. Falls Church, Va. 22046 (10 copies)	Naval Electronic Systems Command Attn: PME-117-22, Cmdr. R. L. Gates Department of the Navy Washington, D.C. 20360
Director Defense Communications Agency Code 960 Washington, D.C. 20305	Naval Electronic Systems Command Attn: PME-117-23, Department of the Navy Washington, D.C. 20360
IIT Research Institute Attn: Mr. A. Valentino, Div. E. 10 W. 35th Street Chicago, Illinois 60616	Naval Electronic Systems Command Attn: PME-117-24, Leroy S. Woznak Department of the Navy Washington, D. C. 20360
Naval Civil Engineering Laboratory Attn: Mr. J. R. Allgood Port Hueneme, CA 93043	Naval Facilities Engineering Command Attn: Mr. G. Hall (Code 054B) Washington, D.C. 20390
Naval Electronics Laboratory Center Attn: Mr. R. O. Eastman San Diego, CA 92152	Naval Research Laboratory A Attn: Mr. Garner 4555 Overlook Ave. S.W. Washington, D.C. 20390
Naval Electronic Systems Command Attn: PME-117T, Mr. J. E. DonCarlos Dept. of the Navy Washington, D.C. 20360 (2 copies)	Naval Research Laboratory Attn: Mr. R. LaFonde 4555 Overlook Ave. S.W. Washington, D.C. 20390
Naval Electronic Systems Command Attn: PME-117-21, Capt. J. Galloway Department of the Navy Washington, D.C. 20360	New London Laboratory Naval Underwater Systems Center Attn: Mr. J. Merrill New London, CT 06320 (4 copies)

The Defense Documentation Center
Attn: DDC-TCA
Cameron Station, Building 5
Alexandria, VA 22314

Naval Research Lab
Attn: Russel M. Brown, Code 5252
4555 Overlook Ave. S.W.
Washington, D. C. 20390

Dr. Philip Karr
Building M3 Room 2946
1 Space Park
Redondo Beach, CA 90278

Dr. A. C. Frazer-Smith
Radioscience Laboratory
Stanford University
Stanford, CA 94305

Dr. E. C. Field
Pacific Sierra Research Corp.
1456 Cloverfield Blvd.
Santa Monica, CA 90404

Capt. W. C. Cobb
Naval Electronic Systems Command
Attn: PME-117
Dept. of the Navy
Washington, D.C. 20360

SECURITY CLASSIFICATION OF THIS PAGE (When Data Entered)

DD FORM 1473 EDITION OF 1 NOV 65 IS OBSOLETE
1 JAN 73

SECURITY CLASSIFICATION OF THIS PAGE (When Data Entered)